

Article

Isolation of Lobane and Prenyleudesmane Diterpenoids from the Soft Coral *Lobophytum varium*

Chuan-Hsiang Chang ^{1,†}, Atallah F. Ahmed ^{2,3,†} , Tian-Sheng Yang ^{1,†}, You-Cheng Lin ⁴,
Chiung-Yao Huang ¹, Tsong-Long Hwang ^{5,6,7}  and Jyh-Horng Sheu ^{1,4,8,9,10,*}

¹ Department of Marine Biotechnology and Resources, National Sun Yat-sen University, Kaohsiung 804, Taiwan; hunter02141991@gmail.com (C.-H.C.); b025020004@student.nsysu.edu.tw (T.-S.Y.); betty8575@yahoo.com.tw (C.-Y.H.)

² Department of Pharmacognosy, College of Pharmacy, King Saud University, Riyadh 11451, Saudi Arabia; afahmed@ksu.edu.sa

³ Department of Pharmacognosy, Faculty of Pharmacy, Mansoura University, Mansoura 35516, Egypt

⁴ Doctoral Degree Program in Marine Biotechnology, National Sun Yat-sen University, Kaohsiung 804, Taiwan; cand93@yahoo.com.tw

⁵ Graduate Institute of Natural Products, College of Medicine, Chang Gung University, Taoyuan 333, Taiwan; htl@mail.cgu.edu.tw

⁶ Research Center for Chinese Herbal Medicine, Research Center for Food and Cosmetic Safety, and Graduate Institute of Health Industry Technology, College of Human Ecology, Chang Gung University of Science and Technology, Taoyuan 333, Taiwan

⁷ Department of Anesthesiology, Chang Gung Memorial Hospital, Taoyuan 333, Taiwan

⁸ Department of Medical Research, China Medical University Hospital, China Medical University, Taichung 404, Taiwan

⁹ Graduate Institute of Natural Products, Kaohsiung Medical University, Kaohsiung 807, Taiwan

¹⁰ Frontier Center for Ocean Science and Technology, National Sun Yat-sen University, Kaohsiung 804, Taiwan

* Correspondence: sheu@mail.nsysu.edu.tw; Tel.: +886-7-5252000 (ext. 5030); Fax: +886-7-5255020

† These authors contributed equally to this work.

Received: 25 March 2020; Accepted: 16 April 2020; Published: 22 April 2020



Abstract: Further chemical investigation of the EtOAc extract of the soft coral *Lobophytum varium* resulted in the discovery of eleven new diterpenoids lobovarols F–P (**1–11**) of lobane- and prenyleudesmane-types, along with two known metabolites (**12** and **13**). The structures of the new metabolites were established by spectroscopic analyses, including 2D NMR experiments. The absolute configuration of **1** was determined using Mosher's method. The complete assignment of ¹H and ¹³C NMR spectroscopic data of **12** and **13** and the identification of pyran-derived moieties in the prenyleudesmanes were reported for the first time. Anti-inflammatory activities of the isolated compounds in suppressing elastase release and superoxide anion generation in human neutrophils were disclosed for **1**, **2**, **4**, **12**, and **13**. A stereospecific biosynthesis for lobanes and prenyleudesmanes from the related prenylgermacranes could explain the coexistence of lobanes and prenylgermacranes in *L. varium*.

Keywords: lobane; prenyleudesmane; anti-inflammatory activity; *Lobophytum varium*

1. Introduction

Soft corals belonging to genus *Lobophytum* (Alcyoniidae) were shown to be the main biological sources of lobane [1–7], prenyleudesmane [1,8–11], and spatane-type diterpenoids [8]. Some lobane and prenyleudesmane diterpenoids have displayed antimicrobial [2], cytotoxic [2,6,8], and anti-inflammatory activities [1]. Cembranoids have also been isolated from this genus, and have been

shown to exhibit significant cytotoxic [12–14], antiviral [15], and anti-inflammatory activities [14,16–18]. Our previous chemical study on the EtOAc extract of a Formosan soft coral, *Lobophytum varium* has led to the discovery of five new metabolites of lobane- and prenyleudesmane-types, of which some were found to possess anti-inflammatory activity through the suppression of elastase release and/or superoxide anion generation in challenged neutrophils [1]. The present study was aimed to further discover new bioactive diterpenoids from continuing investigation of the organic fractions of *L. varium*. This study not only led to the isolation of new metabolites but also gave strong evidence for the biosynthetic mechanism of lobane and prenyleudesmane from the corresponding prenylgermacrane biosynthetic intermediate was proposed, which could explain the common coexistence of lobane and prenylgermacranes in *L. varium*.

2. Results and Discussion

The terpenoids containing fractions of the EtOAc extract of *L. varium* were repeatedly purified using a series of chromatographic techniques, including HPLC, to afford compounds 1–13 (Figure 1). The structures of the new compounds (1–11) were established on the basis of NMR data (Tables 1–3) and spectroscopic analyses (Supplementary Materials, Figures S1 to S79).

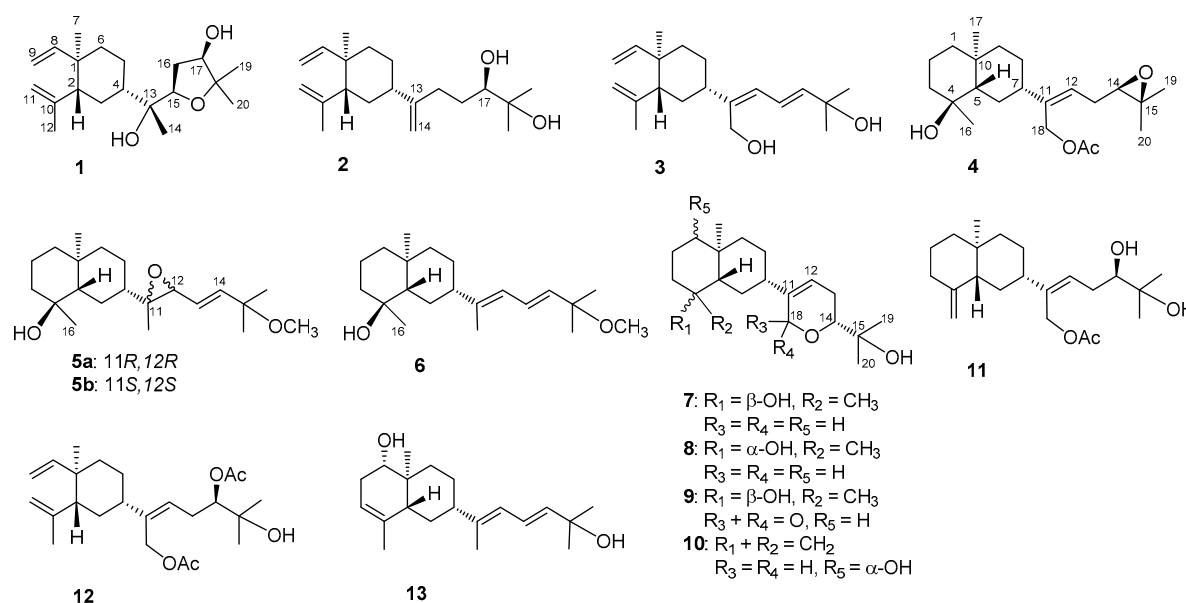


Figure 1. Structures of compounds 1–13.

Lobovarol F (**1**) was found to possess a molecular formula C₂₀H₃₄O₃ as established by high-resolution electrospray ionization mass spectrometry (HRESIMS, *m/z* 345.2403, [M + Na]⁺), indicating four degrees of unsaturation. The IR absorption at 3393 cm^{−1} designated the presence of the hydroxy group. The NMR signals (Table 1) showed the presence of a vinyl (δ_C 150.0, CH and 110.0, CH₂; δ_H 5.80, dd, *J* = 18.0, 10.4 Hz, 4.90 d, *J* = 10.4 Hz, and 4.89, br d, *J* = 18.0 Hz), an isopropenyl (δ_C 147.6, C; 112.1, CH₂ and 24.9, CH₃; δ_H 4.83 and 4.59, each 1H, s; and 1.71, 3H, s); a ring-juncture methyl (δ_C 16.6, CH₃; δ_H 0.99, 3H, s) and methine (δ_C 52.4, CH; δ_H 1.98, m) of a β-elemene segment of lobane-type diterpenoids [1–3]. Thus, the proton signals at δ_H 1.30, 1.26, and 1.15 (each 3H, s) should be the methyls attached to the oxygen-bearing carbons of the side chain. The analysis of correlations spectroscopy (COSY) and heteronuclear multiple bond correlation (HMBC) led to the establishment of a 2,2-dimethyl-3-hydroxytetrahydrofuran attached to a methyl-bearing oxygenated carbon (δ_C 75.0, C-13) to form the side chain of **1** (Figure 2). Accordingly, the HMBC correlations from H₃-14 (δ_H 1.26) and from both H₃-19 and H₃-20 (δ_H 1.15 and 1.30) to the downfield shifted oxycarbons (δ_C 80.4, CH and 84.0, C), respectively, assigned the 15,18-ether linkage of the tetrahydrofuran ring. Moreover, the

HMBC correlations observed from H₃-14 and from both of H₃-19 and H₃-20 to oxycarbons (δ_C 75.0, C and 76.6, CH) positioned the two hydroxy groups at C-13 and C-17, respectively.

The relative configurations of **1** at C-1, C-2, C-4, C-13, C-15, and C-17 were assigned by the nuclear Overhauser effect spectroscopy (NOESY) correlation analysis (Figure 3a) and supported by MM2 force-field modeling and NMR data. From the NOE correlations displayed for H₃-7/H₃-12 and H-2/H-4 and by comparison of the chemical shifts of C-1 to C-12 with those of the previously reported lobane-type diterpenoids [1,2,5,6,19], the 1*R**,2*R**,4*S** configurations of **1** was determined. Moreover, H₃-14 and H-15 showed the NOE interactions with the β -oriented H-4 and H₂-5, leading to the assignment of the corresponding β - and α -orientations of H₃-14 and H-15, respectively. The α -orientation for the hydroxy group at C-13 was thus suggested and also supported by the down-field shifted H-3 (δ_H 1.70, m) relative to those of lobane-type diterpenoids having a β -orientated hydroxy group [1]. A conformation analysis for **1** and its 13-epimer, using MM2 calculations and measuring distances between protons showing key NOEs, also revealed the α -orientation of 13-OH, as the distances between both H-15/H₂-5 and H-4/H₃-14 were found to be shorter than 2.8 Å in **1**. Furthermore, the NOE correlations between H₃-19 (δ_H 1.15, 3H, s) and both H-15 and H-17 disclosed the β -orientations of the hydroxy at C-17. The *R**-configurations for C-13, C-15, and C-17 were thus assigned. By using Mosher's method [20,21], the absolute *R* configuration for C-17 was proven by the analysis of the calculated $\Delta\delta$ ($\delta_S - \delta_R$) values of the neighboring protons to C-17 from the ¹H NMR data of 17-(*S*)- and 17-(*R*)- α -methoxy- α -(trifluoromethyl)phenylacetyl (MTPA) esters of **1** (**1a** and **1b**), respectively (Figure 3b). Based on the above findings, lobovarol F (**1**) was determined to be (1*R*,2*R*,4*S*,13*R*,15*R*,17*R*)-15,18-epoxyloba-8,10-dien-13,17-diol. To the best of own knowledge, **1** is the first lobane diterpene with a tetrahydrofuran-containing side chain.

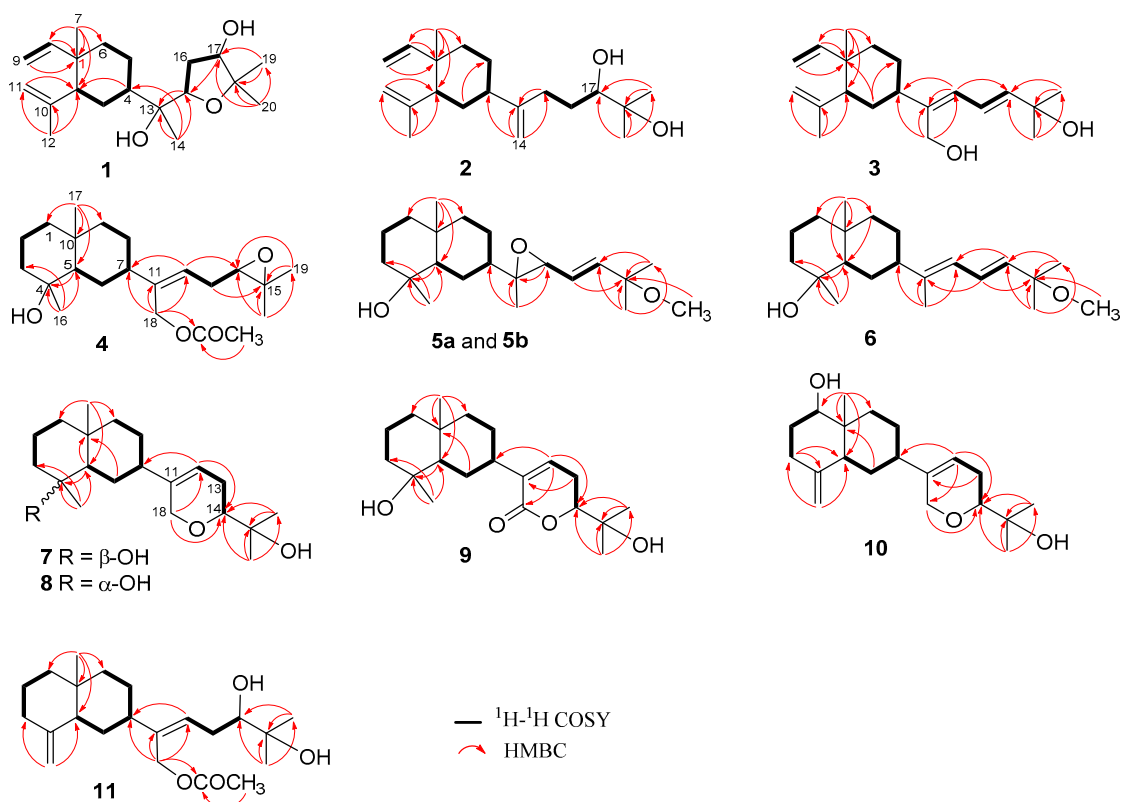


Figure 2. ¹H-¹H COSY and HMBC correlations of 1-11.

Table 1. ^{13}C and ^1H NMR spectroscopic data of compounds 1–4.

Position	1		2		3		4	
	δ_{C}^a (Mult.) ^b	δ_{H}^c (J in Hz)	δ_{C}^a (Mult.)	δ_{H}^c (J in Hz)	δ_{C}^d (Mult.)	δ_{H}^e (J in Hz)	δ_{C}^a (Mult.)	δ_{H}^c (J in Hz)
1	39.9, C		39.8, C		39.7, C		41.0, CH ₂	1.38 m; 1.08 m
2	52.4, CH	1.98 m	52.8, CH	2.01 m	52.8, CH	2.04 dd (7.5, 7.5)	20.1, CH ₂	1.55–1.15 m
3	27.4, CH ₂	1.70 m; 1.50 m	33.3, CH ₂	1.58 m	33.4, CH ₂	1.60 m	43.4, CH ₂	1.80 d (13.2); 1.40 m
4	45.1, CH	1.52 m	44.4, CH	1.93 m	43.6, CH	2.20 m	72.2, C	
5	23.1, CH ₂	1.35 m; 1.24 m	27.4, CH ₂	1.66 m; 1.47 m	27.2, CH ₂	1.64 m; 1.52 m	54.9, CH	1.27 m
6	39.7, CH ₂	1.42 m	39.7, CH ₂	1.52 m; 1.47 m	39.9, CH ₂	1.50 m	27.2, CH ₂	1.52 m
7	16.6, CH ₃	0.99 s	16.6, CH ₃	1.01 s	16.6, CH ₃	1.02 s	44.7, CH	2.06 m
8	150.0, CH	5.80 dd (18.0, 10.4)	150.2, CH	5.82 dd (17.2, 10.8)	150.1, CH	5.82 dd (17.5, 11.5)	26.4, CH ₂	1.85 d (12.0); 1.22 m
9	110.0, CH ₂	4.90 d (10.4) 4.89 br d (18.0)	110.0, CH ₂	4.90 d (17.2) 4.90 d (10.8)	110.0, CH ₂	4.92 d (11.5) 4.89 d (17.5)	44.6, CH ₂	1.45 m 1.21 m
10	147.6, C		147.6, C		147.5, C		34.6, C	
11	112.1, CH ₂	4.83 s; 4.59 s	112.1, CH ₂	4.59 s; 4.82 br s	112.2, CH ₂	4.82 s; 4.59 s	141.0, C	
12	24.9, CH ₃	1.71 s	24.8, CH ₃	1.71 s	24.8, CH ₃	1.71 s	124.7, CH	5.58 dd (8.0, 6.8)
13	75.0, C		154.5, C		145.3, C		27.9, CH ₂	2.39–2.30 m
14	20.4, CH ₃	1.26 s	107.4, CH ₂	4.82 s 4.77 s	60.0 CH ₂	4.31 d (12.5) 4.29 d (12.5)	63.7 CH	2.76 dd (6.4, 6.4)
15	80.4, CH	4.01 dd (9.2, 4.0)	32.0, CH ₂	2.35 m; 2.12 m	126.1, CH	6.02 d (11.0)	58.6, C	
16	34.3, CH ₂	2.39 ddd (14.4, 9.2, 6.0) 1.95 dd (14.4, 4.0)	30.0, CH ₂	1.64 m 1.47 m	121.9, CH	6.61 dd (15.0, 11.0)	22.7, CH ₃	1.12 s
17	76.6, CH	3.78 br d (6.0)	78.4, CH	3.78 d (10.8)	142.0, CH	5.88 d (15.0)	18.7, CH ₃	0.90 s
18	84.0, C		73.1, C		70.9, C		61.2, CH ₂	4.62 d (12.0); 4.61 d (12.0)
19	25.5, CH ₃	1.15 s	23.3, CH ₃	1.18 s	29.8, CH ₃	1.36 s	24.8, CH ₃	1.33 s
20	22.2, CH ₃	1.30 s	26.5, CH ₃	1.23 s	29.8, CH ₃	1.36 s	18.7, CH ₃	1.31 s
Ac							171.0, C 21.1, CH ₃	2.06 s

^a Spectrum recorded at 100 MHz in CDCl₃. ^b Attached protons were deduced by the distortionless enhancement by polarization transfer (DEPT) experiment. ^c Spectrum recorded at 400 MHz in CDCl₃. ^d Spectrum recorded at 125 MHz in CDCl₃. ^e Spectrum recorded at 500 MHz in CDCl₃.

Table 2. ^{13}C and ^1H NMR spectroscopic data of compounds 5–8.

Position	5a + 5b		6		7		8	
	δ_{C}^a (Mult.) ^b	δ_{H}^c (J in Hz)	δ_{C}^d (Mult.)	δ_{H}^e (J in Hz)	δ_{C}^d (Mult.)	δ_{H}^e (J in Hz)	δ_{C}^d (Mult.)	δ_{H}^e (J in Hz)
1	42.1, CH ₂	1.37 m; 1.06 m	41.0, CH ₂	1.42 m; 1.11 m	41.0, CH ₂	1.40 m; 1.07 m	41.5, CH ₂	1.44 m; 1.08 m
2	20.9, CH ₂	1.53 m; 1.49 m	20.1, CH ₂	1.58 m; 1.55 m	20.1, CH ₂	1.58-1.53 m	18.0, CH ₂	1.85 m; 1.65 m
3	44.3, CH ₂	1.71 m	43.3, CH ₂	1.82 m; 1.38 m	43.4, CH ₂	1.78 br d (12.0); 1.38 m	41.3, CH ₂	1.69 m; 1.44 m
4	71.4, C		72.2, C		72.2, C		71.9, C	
5	55.2/55.3, CH	1.21 m	54.9, CH	1.25 m	54.9, CH	1.25 m	51.8, CH	1.07 m
6	23.8/23.9, CH ₂	1.54 m	26.5, CH ₂	1.53 m; 1.51 m	26.0, CH ₂	1.86 br d (9.2); 1.14 m	25.7, CH ₂	1.70 m; 1.34 m
7	48.2/48.3, CH	1.20 m	48.3, CH	2.01 m	42.5, CH	1.86 br d (9.2)	42.9, CH	1.85 m
8	23.0, CH ₂	2.00 m	25.8, CH ₂	1.81 m; 1.26 m	27.0, CH ₂	1.48 m; 1.42 m	27.3, CH ₂	1.48 m
9	45.2, CH ₂	1.41 m; 1.16 m	44.6, CH ₂	1.47 m; 1.22 m	44.6, CH ₂	1.42 m; 1.19 m	43.8, CH ₂	1.36 m; 1.14 m
10	35.4, C		34.6, C		34.6, C		33.7, C	
11	65.7, C		143.4, C		141.4, C		141.5, C	
12	62.6/62.8, CH	3.24/3.26 d (7.0)	122.5, CH	5.90 d (10.8)	116.3, CH	5.57 br d (5.6)	116.4, CH	5.59 br d (4.0)
13	126.3/126.4, CH	5.557/5.563 dd (16.0, 7.0)	126.0, CH	6.39 dd (15.6, 10.8)	25.3, CH ₂	2.14 br d (13.6, 12.8)	25.3, CH ₂	2.16 m
14	141.7/141.8, CH	5.84 d (16.0)	136.6 CH	5.57 d (15.6)	80.3 CH	3.26 dd (11.2, 3.6)	80.3 CH	3.27 dd (10.8, 3.2)
15	75.1, C		75.1, C		71.1, C		71.7, C	
16	23.1, CH ₃	1.07 s	22.7, CH ₃	1.12 s	22.7, CH ₃	1.11 s	30.3, CH ₃	1.15 s
17	19.1, CH ₃	0.90 s	18.7, CH ₃	0.90 s	18.6 CH ₃	0.88 s	18.6, CH ₃	1.04 s
18	14.3/14.4, CH ₃	1.23 s	15.3, CH ₃	1.80 s	68.2, CH ₂	4.18 d (16.4)	68.2, CH ₂	4.19 d (16.4)
19	26.0/26.1, CH ₃	1.24 s	26.0, CH ₃	1.30 s	26.1, CH ₃	4.23 d (16.4)	26.1, CH ₃	4.21 d (16.4)
20	26.3/26.4, CH ₃	1.24 s	26.0, CH ₃	1.30 s	23.6, CH ₃	1.21 s	23.6, CH ₃	1.17 s
OCH ₃	50.4, CH ₃	3.10 s	50.4, CH ₃	3.18 s		1.17 s		

^a Spectrum recorded at 125 MHz in acetone-d₆. ^b Attached protons were deduced by the DEPT experiment. ^c Spectrum recorded at 500 MHz in acetone-d₆. ^d Spectrum recorded at 100 MHz in CDCl₃. ^e Spectrum recorded at 400 MHz in C.

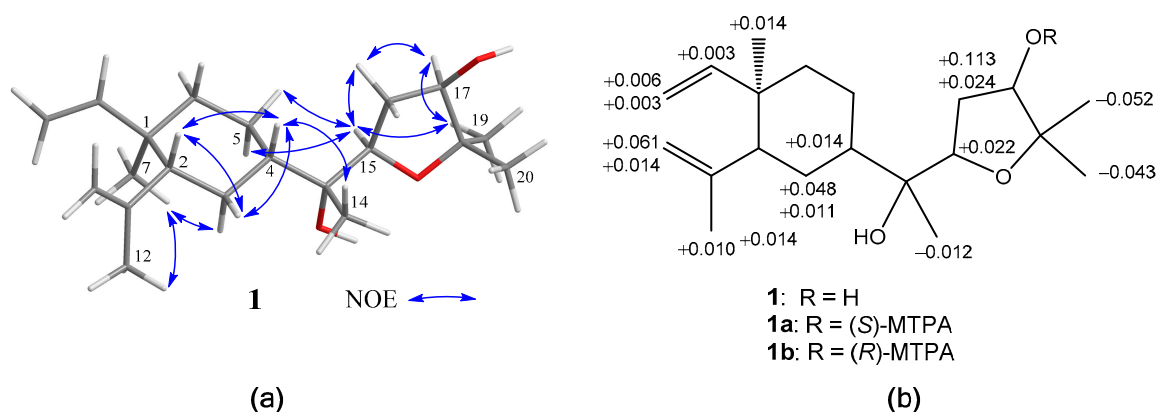


Figure 3. (a) Key nuclear Overhauser effect (NOE) correlations of **1**; (b) ^1H NMR chemical shift differences $\Delta(\delta_S - \delta_R)$ in ppm for the MTPA esters of **1**.

Lobovarol G (**2**) displayed a sodiated ion peak at m/z 329.2453 in the HRESIMS spectrum, appropriate for a molecular formula $\text{C}_{20}\text{H}_{34}\text{O}_2$. The IR absorption at 3392 cm^{-1} also indicated the presence of hydroxy group. The NMR data of **2** (Table 1) showed resonances and coupling patterns identical to those of the β -elemene ring system in **1** as well as other lobane-type diterpenoids [1–7]. The fourth degree of unsaturation has arisen from an 1,1-disubstituted double bond (δ_C 154.5, C and 107.4, CH_2 ; and δ_H 4.82 and 4.77, each 1H, s). NMR data showed that **2** differs with (1*R*,2*R*,4*S*,17*R*)-loba-8,10,13(15)-trien-17,18-diol, isolated from the same organism (*L. varium*) [1] and *L. pauciflorum* [2], only in the position of the double bond of the side chain. The analysis of HMBC correlations further confirmed the C-17 and C-18 positions of the hydroxy groups in the side chain (Figure 2). Compound **2** should possess the same 1*R*,2*R*,4*S*-configuration of the β -elemene ring system as that of **1** by the biogenetic relationship with **1** and the previously reported lobane diterpenoids isolated from genus *Lobophytum* [1,5,19]. Comparison of NMR data of the side chain of **2** (Table 1) with the corresponding data of chokol E (**14**) [22] and 10-*epi*-chokol E (**15**) [23] of known absolute configurations (Figure 4), allowed the elucidation of 17*R** configuration in **2**. As **1** and **2** should share the same biosynthetic pathway, therefore, the structure of **2** was suggested to be (1*R*,2*R*,4*S*,17*R*)-loba-8,10,13-trien-17,18-diol.

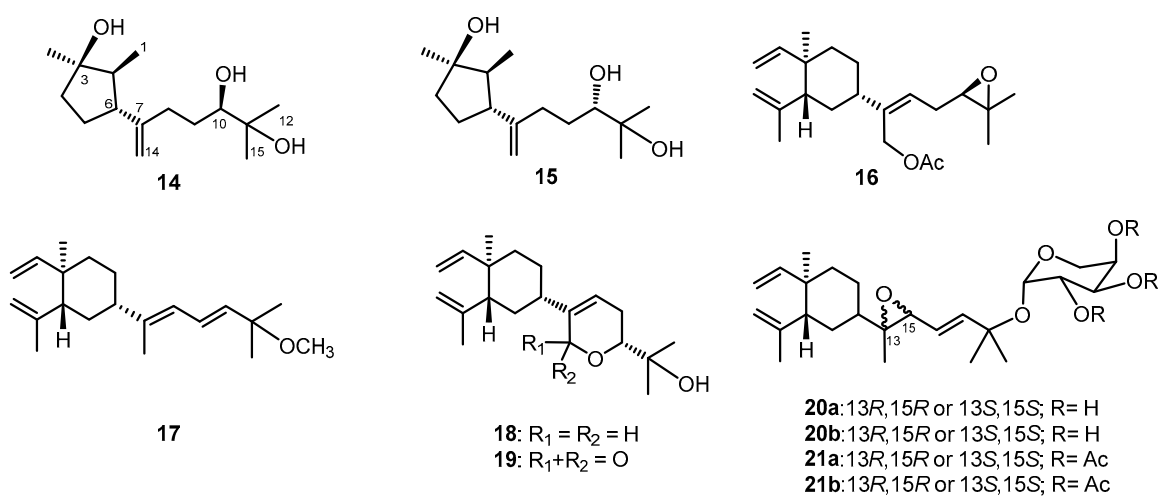


Figure 4. Known sesquiterpenoids chokol E (**14**) and 10-*epi*-chokol E (**15**); lobane diterpenoids (**16–19**); fuscoides C and D (**20a** and **20b**), and fuscoides C and D acetates (**21a** and **21b**).

Lobovarol H (**3**) possessed a molecular formula $C_{20}H_{32}O_2$ (HRESIMS: m/z 327.2294 $[M + Na]^+$) and showed the presence of hydroxy and olefinic functionalities from the IR absorptions at 3352 and 1645 cm^{-1} . The NMR data (Table 1) revealed that **3** is a lobane diterpenoid, with the presence of a trisubstituted (δ_C 145.3, C and 126.1, CH; δ_H 6.02, d, $J = 11.0$ Hz) and an 1,2-disubstituted double bond (δ_C 142.0, CH and 121.9, CH; δ_H 6.61, dd, $J = 15.0, 11.0$ Hz and 5.88, d, $J = 15.0$ Hz); and hydroxymethylene group (δ_C 60.0 CH_2 ; δ_H 4.31 and 4.29, each 1H, d, $J = 12.5$ Hz) in the side chain.

The NMR data of the side chain of **3** was found to be the same as the corresponding data of known compound **13** except the olefinic methyl of **13** was replaced by a hydroxymethylene group (δ_H 4.31 and 4.29, each 1H, d, $J = 12.5$ Hz) in **3**. The HMBC correlations of **3** further confirmed the C-13, C-13/C-15, C-16/C-17, and C-18 positions of the hydroxymethylene, two conjugated double bonds, and a hydroxy group, respectively (Figure 2). Finally, the strong NOE correlation of H₂-14/H-16 and the large J value of H-16 and H-17 (15.0 Hz) determined the *Z* and *E* configurations of C-13/C-15 and C-16/C-17 double bonds, respectively. Compound **3** was thus established as (1*R*,2*R*,4*S*,13*Z*,16*E*)-loba-8,10,13(15),16-tetraen-14,18-diol.

Lobovarol I (**4**) displayed a sodiated ion peak $[M + Na]^+$ at m/z 387.2504 in the HRESIMS, appropriate for a molecular formula $C_{22}H_{36}O_4$, and five degrees of unsaturation. The IR absorptions at 3278 and 1740 cm^{-1} revealed the presence of the hydroxy and ester carbonyl groups. The NMR data (Table 1) showed the presence of a trisubstituted double bond (δ_C 141.0, C and 124.7, CH; δ_H 5.58, dd, $J = 8.0, 6.8$ Hz), a trisubstituted epoxide (δ_C 58.6, C; 63.7, CH; δ_H 2.76, 1H, dd, $J = 6.4, 6.4$ Hz), and an acetoxy group (δ_C 171.0, C; 21.1 CH_3 ; δ_H 2.06, 3H, s). The remaining two degrees of unsaturation have arisen from the presence of two rings. A decalin bicarbocyclic structure with an angular methyl (δ_H 0.90, 3H, s) and a methine (δ_C 54.9, CH; δ_H 1.27, m) was elucidated from the COSY and HMBC correlations (Figure 2) which showed **4** to be a prenyleudesmane type diterpene [9,10]. The C-4 position of the hydroxy group was confirmed from the HMBC correlation of H₃-16 (δ_H 1.12, s,) to C-5 (δ_C 54.9, CH) and C-4 (δ_C 72.2, C). Moreover, the NMR data of the side chain of **4** were found to be identical in all aspects to those of the side chain of acetoxylobaoxide (**16**) (Figure 4) [5], the gross structure of **4** was thus established unambiguously.

The relative configuration of **4** was determined based on biogenetic consideration, NOESY correlations (Figure 5a) and NMR data comparison of related metabolites. Accordingly, the steric orientations of H₃-17, H-5, and H-7 in the bicarbocyclic ring system of prenyleudesmanes **4** and **5–11** (*vide infra*) should be α , β , and β , respectively, as the same with the corresponding H₃-17, H-2, and H-4 of the ring system of the lobanes (**1–3**), as the showed by the NOESY analysis of lobovarol I (**4**) (Figure 5a). Consequently, the NOE interaction displayed between H₃-17 and H₃-16 indicated the β -orientation of the hydroxy group at C-4. Furthermore, the NMR data of the side chain in **4** were identical to those of the side chain in acetoxylobaoxide (**16**), of which the *R* absolute configuration at C-14 has been determined after reduction of the C-14/C-15 epoxide [5]. From the above results, the structure of **4** was determined as (4*S*,5*S*,7*S*,10*S*,11*Z*,14*R*)-14,15-epoxy-18-acetoxyprenyleudesma-11-en-4-ol.

Lobovarol J (**5a** and **5b**) were obtained as an inseparable mixture ($\approx 1:1$) of two isomers as revealed from the NMR spectra which displayed two sets of signals with an only slight difference in the chemical shifts for certain carbon and proton atoms. The HRESIMS (m/z 359.2555 $[M + Na]^+$) was determining a molecular formula ($C_{21}H_{36}O_3$) for the mixture of two isomers. Comparison of the NMR data of **5a** and **5b** (Table 2) with those of **4** (Table 1) revealed that lobovarol J possessed the same bicarbocyclic system as that of **4** (Table 2) and the similar side chain of fuscoides C & D triacetates (**21a** and **21b**) [24], except that the sugar moiety in **21a** or **21b** (Figure 4) was replaced by a methoxy group (δ_C 50.4, CH_3 ; δ_H 3.10, 3H, s) in **5**. The planar structure of **5a** and **5b** was then established, as illustrated in Figure 2. The *E* configuration of the 13,14-double bond and the *trans* 11,12-epoxide were deduced from the J values of H-13 and H-14 (16.0 Hz) and the NOE correlations (Figure 5b), respectively. However, by using MM2 calculation for either stable conformation of **5a** or **5b**, it was found that either isomer showed a distance of near 2.4 Å between the NOE-interacting protons H-12 and H-7 (Figure 5b). Therefore, the two new compounds were defined as 11*R*,12*R*- (**5a**) and 11*S*,12*S*-

(5b) isomers of (4*S*,5*S*,7*S*,10*S*,13*E*)-11,12-epoxy-15-methoxyprenyleudesma-13-en-4-ol with the exact NMR spectroscopic data for each isomer remained for further elucidation.

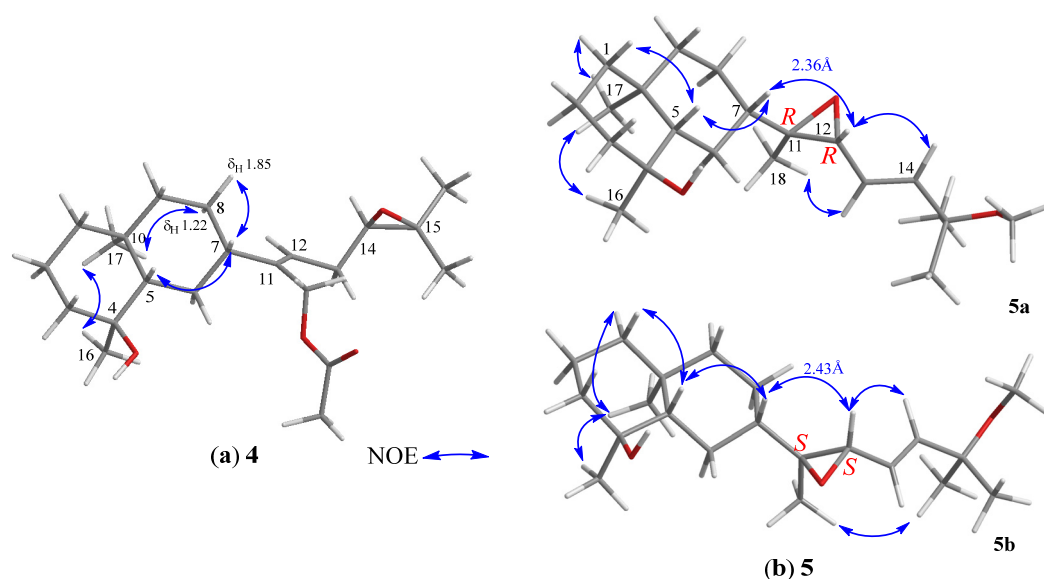


Figure 5. (a) Selected NOE correlations of **4**; (b) Selected NOE correlations of 11,12-bisepimers.

Lobovarol K (**6**) has a molecular formula $C_{21}H_{36}O_2$, as displayed from the sodiated ion peak in the HRESIMS (m/z 343.2606 [$M + Na$] $^+$), and showed the presence of a hydroxy group (IR 3431 cm^{-1}). The NMR spectroscopic data of **6** (Table 2) are similar to a methoxylated (δ_C 50.4, CH_3 and δ_H 3.18, 3H, s) prenyleudesmane, including signals of five methyls. The 1H and ^{13}C NMR data of **6** further revealed that it is a diterpene possessing the same side chain as that of lobane **17** [2]. The chemical shifts of C-18 (δ_C 15.3, CH_3) and J value of H-13 and H-14 (15.6 Hz) indicated the *E*-geometry for the 11,12- and 13,14-double bonds, respectively. The NOE correlations (Figure 6a) and the above-mentioned biogenetic consideration established **6** as (4*S*,5*S*,7*S*,10*S*,11*E*,13*E*)-15-methoxyprenyleudesma-11,13-dien-4-ol.

Lobovarol L (**7**) possessed a molecular formula $C_{20}H_{34}O_3$ (HRESIMS m/z 345.2401 [$M + Na$] $^+$). Compound **7** displayed the combined NMR data of the eudesmane ring system in **4–6** (Table 2), and the side chain of lobatriene (**18**) [19]. The planar structure was further established by the analysis of COSY and NMR correlations (Figure 2). The configuration of **7** was established after the structure determination of **8**. NOE correlations between the known α -oriented H_3 -17 and H_3 -16, and β -oriented H-7 with H-5, but not between H-5 and both H_3 -16 and H_3 -17 led to the structure of **7** to be determined as shown in formula **7**.

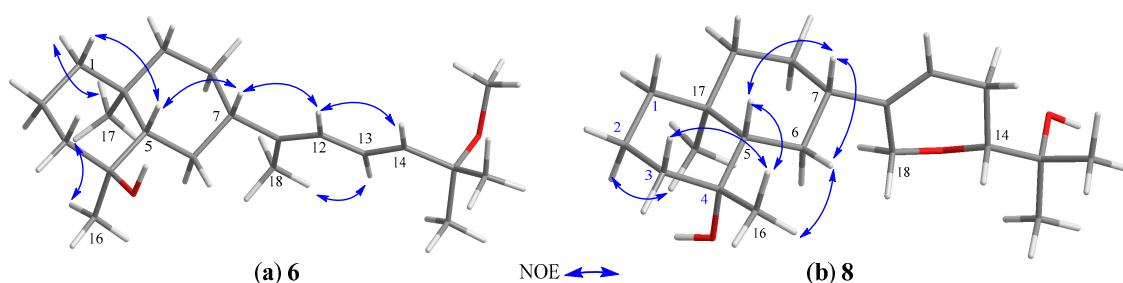


Figure 6. (a) Selected NOE correlations of **6**; (b) selected NOE correlations of **8**.

The HRESIMS of lobovarol M (**8**) showed the same molecular formula $C_{20}H_{34}O_3$ as that of **7**, suggesting **8** to be an isomer for **7**. The NMR data of **8** were found to be very similar to those of **7** (Table 2); however, **8** exhibited more upfield chemical shifts for carbons around C-4, in particular

C-2, C-3, and C-5 ($\Delta\delta_C$ -2.1 , -2.1 , and -3.1 , respectively) relative to the correspondent carbons in **7**, supporting that **8** is the 4-epimer of **7**. Unlike the NOE correlations of **7**, **8** exhibited correlations (Figure 6b) between H₃-17 and H-2 α , but not between H₃-17 and H₃-16. Also, H₃-16 showed NOE interactions with both H-3 β and H-5, and H-5 displayed correlation with the β -oriented H-7, thus **8** was determined as 4-epimer of **7**.

Table 3. ¹³C and ¹H NMR spectroscopic data of compounds **9–11**.

Position	9		10		11	
	δ_C^a (Mult.) ^b	δ_H^c (J in Hz)	δ_C^d (Mult.)	δ_H^e (J in Hz)	δ_C^d (Mult.)	δ_H^e (J in Hz)
1	40.9, CH ₂	1.40 m; 1.10 m	79.2, CH	3.42 dd (11.5, 4.0)	41.8, CH ₂	1.44 m; 1.28 m
2	20.1, CH ₂	1.56 m	31.4, CH ₂	1.82 m; 1.56 m	23.4, CH ₂	1.63 m
3	43.6, CH ₂	1.83 m; 1.80 m	34.1, CH ₂	2.32 m; 2.11 m	36.8, CH ₂	2.31 m; 2.01 m
4	72.1, C		148.5, C		150.7, C	
5	54.9, CH	1.32 m	47.5, CH	1.77 m	49.9, CH	1.83 d (11.5)
6	25.4, CH ₂	1.90 m	28.8, CH ₂	1.64 m; 1.31 m	29.7, CH ₂	1.56 m; 1.26 m
7	39.5, CH	2.57 m	41.2, CH	1.83 m	44.0, CH	2.01 m
8	27.9, CH ₂	1.67 m; 1.30 m	26.7, CH ₂	1.59 m; 1.42 m	27.5, CH ₂	1.60 m; 1.42 m
9	44.6, CH ₂	1.43 m; 1.34 m	36.9, CH ₂	1.94 m; 1.20 m	41.2, CH ₂	1.51 m; 1.42 m
10	34.6, C		40.2, C		35.9, C	
11	137.2, C		141.2, C		141.6, C	
12	136.7, CH	6.63 d (5.6)	116.4, CH	5.58 d (5.5)	126.6, CH	5.61 t (7.5)
13	24.5, CH ₂	2.49 m; 2.36 m	25.3, CH ₂	2.17 m; 1.96 m	30.4, CH ₂	2.32 m
14	83.3, CH	4.13 dd (12.8, 3.6)	80.3, CH	3.28 dd (11.0, 3.5)	77.6, CH	3.42 m
15	71.0, C		71.7, C		72.7, C	
16	22.5, CH ₃	1.12 s	107.0, CH ₂	4.76 s; 4.50 s	105.5, CH ₂	4.71 s; 4.42 s
17	18.7, CH ₃	0.91 s	10.2, CH ₃	0.70 s	16.4, CH ₃	0.73 s
18	164.7, C		68.2, CH ₂	4.20 br s	61.6, CH ₂	4.54 d (12.0) 4.76 d (12.0)
19	24.4, CH ₃	1.25 s	23.7, CH ₃	1.17 s	23.8, CH ₃	1.20 s
20	25.9, CH ₃	1.33 s	26.1, CH ₃	1.22 s	26.3, CH ₃	1.24 s
Ac					171.3, C	
					21.1, CH ₃	2.06 s

^a Spectrum recorded at 100 MHz in CDCl₃. ^b Attached protons were deduced by the DEPT experiment. ^c Spectrum recorded at 400 MHz in CDCl₃. ^d Spectrum recorded at 125 MHz in CDCl₃. ^e Spectrum recorded at 500 MHz in CDCl₃.

Lobovarol N (**9**) displayed a sodiated ion peak at m/z 359.2191 [M + Na]⁺ in the HRESIMS spectrum of a molecular formula C₂₀H₃₂O₄ and IR absorptions at 3430 and 1700 cm⁻¹ of the hydroxy and ester carbonyl functionalities. The ¹³C and ¹H NMR data (Table 3) were similar to those of **7** except the replacement of the 18-hydroxymethylene signals (δ_C 68.2, CH₂; δ_H 4.23 and 4.18, each br d, J = 16.4 Hz) in **7** by a signal at δ_C 164.7 (C) in **9**. Thus, **9** is the 16-oxo derivative of **7**. The NMR data of the side chain of **9** are also nearly identical with those of lobatrienolide (**19**) [5] coexisting in the same organism [1]. A combination of 2D NMR analyses (Figure 2) and biogenetic relationship with the coexisting biogenetically related lobanes **1,19** [5], and 17,18-epoxyloba-8,10,13(15)-trien-16-ol [1] with confirmed absolute configurations established the structure of **9** as (4*S*,5*S*,7*S*,10*S*,11*Z*,14*R*)-14,18-epoxyprenyleudesma-11-en-4,15-diol-18-one.

The sodium adduct ion peak [M + Na]⁺ of lobovarol O (**10**) at m/z 343.2242 in the HRESIMS showed a molecular formula C₂₀H₃₂O₃ of **10**. NMR data (Table 3) of **10** showed that it has the same cyclic ether ring as **7**, **8**, and lobatriene (**18**) [19] in the side chain. In comparison of the NMR spectroscopic data of **10** (Table 3) with those of **7** and **8** (Table 2) and analysis of COSY spectrum which showed the proton sequence of H-1 (δ_H 3.42, dd, J = 11.5, 4.0 Hz) to H-3 and the HMBC correlations of H₃-17 (δ_H 0.70, 3H, s) to C-1 (δ_C 79.2), C-5 (δ_C 47.5), C-9 (δ_C 36.9), and C-10 (δ_C 40.2), confirmed the presence of a hydroxy group at C-1 and the prenyleudesmane molecular skeleton of **10**. Furthermore, NOE correlations of H-1 with the β -oriented H-5 and one proton of H₂-9 (δ_H 1.20, m) showed the β -orientation of H-1 and this H-9. The other proton at C-9 (δ_H 1.94, m) was thus assigned as H-9 α which exhibited NOE correlation with H₃-17, but not with both H-1 and H-5, thus H₃-17 was assigned as α -oriented.

Lobovarol P (**11**) has the molecular formula C₂₂H₃₆O₄ (HRESIMS: m/z 387.2504 [M + Na]⁺). The NMR data (Table 3) revealed that it possesses the same decalin bicyclic structures [10] and the same

side-chain [3] of known compounds. The gross structure of **11** was thus determined and the relative configuration of **11** was further established by analysis of the NOESY spectrum which exhibited NOE interactions of the β -oriented H-5 (δ_{H} 1.83, d, $J = 11.5$ Hz) with both H-1 β (δ_{H} 1.28, m) and H-7 (δ_{H} 2.10, m), and H-1 α (δ_{H} 1.28, m) with H₃-17 (δ_{H} 0.73, 3H, s). Thus, H-7 was determined to be positioned on the β face. By the biogenetic consideration, lobovarol P was found to possess (5*R*,7*S*,10*S*)-configuration, the same as that of lobovarol E [1].

Although 5,6-dihydro-2H-pyran and 5,6-dihydro-2H-pyran-2-one moieties have been known to be present in the side chain of lobane diterpenoid isolated from genus *Lobophytum* [1–3,5], this is the first report about discovering both pyran and pyranone systems in the structures of prenyleudesmanes. The structures of two known compounds loba-8,10,13(15)-trien-14,17,18-triol-14,17-diacetate (**12**) [3] and the eudesmane derivative (**13**) [9] were established mainly based on the MS and partial ¹H NMR data. The detailed 1D and 2D NMR spectroscopic analysis enabled us to fully assign the ¹H and ¹³C NMR data of these two diterpenoids for the first time.

Cytotoxicity for compounds **1**, **2**, **4**, **7**, **8**, **12**, and **13** against the growth of human colon adenocarcinoma (DLD-1), human colon carcinoma (HT-29), and human liver bile duct carcinoma (HuCCT-1); and for **3**, **5**, **6**, and **9–11** against DLD-1 and mouse lymphocytic leukemia (P388) cancer cell lines using the Alamar Blue assay has been screened [25,26]. The results showed that all of the tested metabolites did not exhibit cytotoxicity towards the above cell lines ($\text{IC}_{50} > 40 \mu\text{g/mL}$) compared to doxorubicin HCl (IC_{50} 0.9–7.4 $\mu\text{g/mL}$).

The anti-inflammatory activities of diterpenoids **2–13** against the fMLF/CB-induced pro-inflammatory responses on human neutrophils were evaluated [27,28], too. The results (Table 4) showed that **12** and **13** have potent inhibitory effect against the elastase release (IC_{50} 6.9 \pm 2.7 and 4.4 \pm 0.7 μM , respectively). Compounds **2** and **4** could suppress elastase release (IC_{50} 18.8 \pm 1.8 and 20.00 \pm 3.0 μM), too, while **13** is the only compound also could significantly suppress the superoxide anion generation (IC_{50} 13.7 \pm 4.4 μM). Thus **2**, **4**, **12**, and **13**, in particular **12** and **13**, have the potential to become anti-inflammatory agents. Compound **1** was found to strongly suppress elastase release in the absence of fMLF/CB, and is worthy for further biological study.

Table 4. Inhibitory effects of compounds **1–13** on the generation of superoxide anion and release of elastase in fMLF/CB-stimulated human neutrophils.

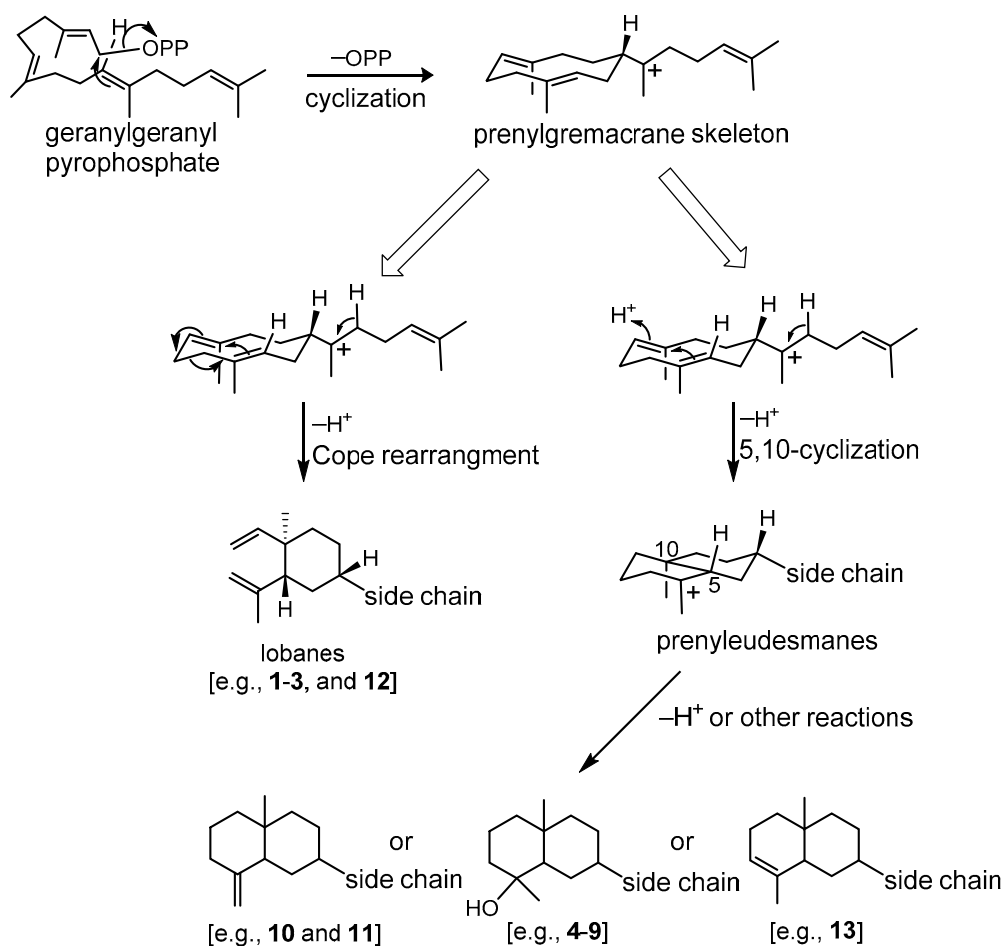
Compound	Superoxide Anion			Elastase Release		
	IC_{50} (μM)	Inh % ^a		IC_{50} (μM)	Inh %	
1	>20	4.6 \pm 3.8 ^b		>20	64.3 \pm 3.7 ^b	
2	>20	18.1 \pm 4.0	*	18.8 \pm 1.8	87.3 \pm 7.9	***
3	>20	4.3 \pm 4.2		>20	3.8 \pm 2.6	
4	>20	40.2 \pm 7.3	**	20.0 \pm 3.0	53.2 \pm 0.2	***
5	>20	8.4 \pm 7.4		>20	3.5 \pm 1.4	
6	>20	4.2 \pm 4.4		>20	−10.9 \pm 5.1	
7	>20	22.9 \pm 7.6	*	NT ^c	NT	
8	>20	19.1 \pm 6.9	*	>20	37.8 \pm 6.2	***
9	>20	5.3 \pm 3.2		>20	5.5 \pm 0.6	***
10	>20	2.7 \pm 5.0		>20	5.3 \pm 1.6	*
11	>20	8.9 \pm 7.0		>20	12.0 \pm 4.4	
12	>20	46.5 \pm 5.8	***	6.9 \pm 2.7	73.7 \pm 2.4	***
13	13.7 \pm 4.4	72.4 \pm 5.9	***	4.4 \pm 0.7	117.3 \pm 3.2	***
Idelalisib ^d	0.07 \pm 0.01		***	0.30 \pm 0.10		***

^a Inh% at 10 $\mu\text{g/mL}$. ^b **1** induced superoxide generation and elastase release in the absence of fMLF/CB. ^c NOT tested.

^d Positive control. Results are presented as mean \pm S.E.M. (n = 3–4). * $p < 0.05$, ** $p < 0.01$, *** $p < 0.001$ compared with the control (DMSO).

Although the structures of lobanes **1–3**, and **12** and eudesmanes **4–11**, and **13**, along with the previously reported related metabolites from the same organism [1] possess different ring structures, they are coexisted in *L. varium* and are biogenetically related to each other

A prenylgermacrene has been regarded as the same biosynthetic precursor [8,9] and we further propose a stereospecific biosynthesis for lobane and prenyleudesmane diterpenoids through Cope rearrangement and acid-catalyzed cyclization, respectively [9,29], as illustrated in Scheme 1. Thus, the co-occurrence of lobanes and prenyleudesmanes could be found in the same soft coral as in the cases of *L. varium* [1], *Lobophytum* sp. [9], *Eunicea fusca* [24], *Simularia gyrosa* [30], and *Simularia polydactyla* [31], is scientifically reasonable.



Scheme 1. Plausible biosynthetic pathway of lobanes and prenyleudesmane-type diterpenoids.

3. Experimental Section

3.1. General Experimental Procedures

Optical rotations and IR spectra were measured on a JASCO P-1020 polarimeter and FT/IR-4100 infrared spectrophotometer (Jasco Corporation, Tokyo, Japan), respectively. ESIMS and HRESIMS experiments were performed on VG Quattro GC/MS and Bruker APEX II mass spectrometers, respectively. The NMR spectra were recorded on a Varian Unity Inova 500 FT-NMR (Varian Inc., Palo Alto, CA, USA) at 500 and 125 MHz for ¹H and ¹³C, respectively; or on a Varian 400 FT-NMR at 400 and 100 MHz for ¹H and ¹³C, respectively. Silica gel 60 or reversed-phase silica gel (RP-18; 230–400 mesh) and precoated silica gel plates (Kieselgel 60 F254, 0.2 mm) (Merck, Darmstadt, Germany) were used for open column chromatography (CC) and analytical TLC analysis, respectively. Isolation and purification of isolates by HPLC were performed by Hitachi L-2455 instrument equipped with an RP-18 column (ODS-3, 5 μm, 250 × 20 mm; Sciences Inc., Tokyo, Japan).

3.2. Amino Material

The soft coral *L. varium* (Tixier-Durivault, 1970) was collected in March 2013 at a depth of 10 to 15 m at Jihui Fish Port, Taitung, Taiwan (23°7'2" N, 121°23'49.2" E) and identified by Professor Chang-Feng Dai, Institute of Oceanography, National Taiwan University, Taipei, Taiwan [1].

3.3. Extraction and Isolation

The sliced frozen soft coral *L. varium* (1.3 kg, wet weight) was exhaustively extracted with EtOAc, and the resulting solvent-free extract (55.40 g) was fractionated by silica gel column chromatography into 24 fractions (F1 to F24) as described before¹. F19 (1.39 g), eluting with 50% EtOAc in *n*-hexane, was permeated through a column of Sephadex LH-20 using acetone to afford two diterpenoid-rich fractions F19-1 (105.0 mg) and F19-2 (94.0 mg). F19-1 was chromatographed over silica gel and eluted with EtOAc–*n*-hexane (1:3) to give two subfractions F19-1a (70.5 mg) and F19-1b (15.0 mg). F19-1a was further divided by reverse phase (RP-18) column chromatography, using MeOH–H₂O, into two subfractions F19-1a1 and F19-1a2 which were purified separately by RP-18 HPLC, using CH₃CN–H₂O (2:1), to yield **1** (2.4 mg) and **2** (3.1 mg) from F19-1a1, and **12** (10.0 mg) from F19-1a2, respectively. F19-1b (15.0 mg) was purified by RP-18 HPLC using CH₃CN–H₂O (1.5:1) to afford **4** (1.1 mg). F19-2 was also primarily chromatographed over silica gel column using EtOAc–*n*-hexane (1:3) where the eluted diterpenoid-rich fraction (50.1 mg) was further isolated by RP-18 column chromatography, using MeOH–H₂O (9:1 then 2:1), to yield **13** (1.4 mg), **7** (1.5 mg), and **8** (4.8 mg), respectively. F20 (1.20 g), eluted with 66.7% EtOAc in *n*-hexane, was fractionated over silica gel column, using EtOAc–*n*-hexane (5:95 to 0:100, gradient), to yield four fractions (F20-1 to F20-4). Isolation of F20-1 over RP-18 silica gel column, using MeOH–H₂O (9:1), gave **5** (2.2 mg) and **6** (3.8 mg), respectively. F20-2 was further separated by RP-HPLC, using MeOH–H₂O (6:1), to afford **10** (2.0 mg) and **11** (3.2 mg), respectively. F21 (0.50 g), eluted with 100% EtOAc, was similarly further fractionated, as for fractionation of F20, to give F21-1 and F21-2. RP-18 silica gel column chromatography was then applied to purify F21-1, using MeOH–H₂O (5:1), to afford **3** (5.0 mg) and to further purify F21-2, using MeOH–H₂O (6:1), to yield **9** (4.0 mg).

Lobovarol F (**1**): Colorless oil; $[\alpha]_D^{24} + 2.8$ (c 2.4, CHCl₃); IR (neat) ν_{\max} 3393, 2926, 1643, 1532, 1462, 1147, 1024, and 897 cm⁻¹; ¹³C and ¹H NMR data (see Table 1); ESIMS m/z 345 [M + Na]⁺; HRESIMS m/z 345.2403 [M + Na]⁺ (calcd for C₂₀H₃₄O₃Na, 345.2400).

Lobovarol G (**2**): Colorless oil; $[\alpha]_D^{24} + 44.5$ (c 3.1, CHCl₃); IR (neat) ν_{\max} 3392, 2926, 2860, 1642, 1523, and 891 cm⁻¹; ¹³C and ¹H NMR data (see Table 1); ESIMS m/z 329 [M + Na]⁺; HRESIMS m/z 329.2453 [M + Na]⁺ (calcd for C₂₀H₃₄O₂Na, 329.2451).

Lobovarol H (**3**): Colorless oil; $[\alpha]_D^{24} - 46.7$ (c 0.57, CHCl₃); IR (neat) ν_{\max} 3352, 2926, 1645, 1456, 1374, and 898 cm⁻¹; ¹³C and ¹H NMR data (see Table 1); ESIMS m/z 327 [M + Na]⁺; HRESIMS m/z 327.2294 [M + Na]⁺ (calcd for C₂₀H₃₂O₂Na, 327.2295).

Lobovarol I (**4**): Colorless oil; $[\alpha]_D^{24} + 66.0$ (c 1.1, CHCl₃); IR (neat) ν_{\max} 3278, 2919, 2852, 1740, and 1531 cm⁻¹; ¹³C and ¹H NMR data (see Table 1); ESIMS m/z 387 [M + Na]⁺; HRESIMS m/z 387.2504 [M + Na]⁺ (calcd for C₂₂H₃₆O₄Na, 387.2506).

Lobovarol J (mixture of **5a** and **5b**): Colorless oil; $[\alpha]_D^{24} + 14.2$ (c 0.63, CHCl₃); IR (neat) ν_{\max} 3443, 2929, 1531, 1456, 1378, and 1068 cm⁻¹; ¹³C and ¹H NMR data (see Table 2); ESIMS m/z 359 [M + Na]⁺; HRESIMS m/z 359.2555 [M + Na]⁺ (calcd for C₂₁H₃₆O₃Na, 359.2557).

Lobovarol K (**6**): Colorless oil; $[\alpha]_D^{24} - 10.9$ (c 0.46, CHCl₃); IR (neat) ν_{\max} 3431, 2922, 1670, 1535, 1458, 1377, and 1071 cm⁻¹; ¹³C and ¹H NMR data (see Table 2); ESIMS m/z 343 [M + Na]⁺; HRESIMS m/z 343.2606 [M + Na]⁺ (calcd for C₂₁H₃₆O₂Na, 343.2608).

Lobovarov L (7): Colorless oil; $[\alpha]_D^{24} + 99.2$ (*c* 1.5, CHCl₃); IR (neat) v_{\max} 3378, 2922, 2852, 1540, 1458, 1089, 906, and 670 cm⁻¹; ¹³C and ¹H NMR data (see Table 2); ESIMS *m/z* 345 [M + Na]⁺; HRESIMS *m/z* 345.2401 [M + Na]⁺ (calcd for C₂₀H₃₄O₃Na, 345.2400).

Lobovarov M (8): Colorless oil; $[\alpha]_D^{24} + 87.7$ (*c* 4.8, CHCl₃); IR (neat) v_{\max} 3459, 2927, 2852, 1451, 1378, 1161, 1088, and 756 cm⁻¹; ¹³C and ¹H NMR data (see Table 2); ESIMS *m/z* 345 [M + Na]⁺; HRESIMS *m/z* 345.2401 [M + Na]⁺ (calcd for C₂₀H₃₄O₃Na, 345.2400).

Lobovarov N (9): Colorless oil; $[\alpha]_D^{24} + 59.7$ (*c* 0.54, CHCl₃); IR (neat) v_{\max} 3430, 2924, 1700, 1429, 1376, and 1096 cm⁻¹; ¹³C and ¹H NMR data (see Table 3); ESIMS *m/z* 359 [M + Na]⁺; HRESIMS *m/z* 359.2191 [M + Na]⁺ (calcd for C₂₀H₃₂O₄Na, 359.2193).

Lobovarov O (10): Colorless oil; $[\alpha]_D^{24} + 48.1$ (*c* 0.57, CHCl₃); IR (neat) v_{\max} 3433, 2926, 1696, 1532, 1024, and 670 cm⁻¹; ¹³C and ¹H NMR data (see Table 3); ESIMS *m/z* 343 [M + Na]⁺; HRESIMS *m/z* 343.2242 [M + Na]⁺ (calcd for C₂₀H₃₂O₃Na, 343.2244).

Lobovarov P (11): Colorless oil; $[\alpha]_D^{24} - 54.0$ (*c* 0.71, CHCl₃); IR (neat) v_{\max} 3503, 2925, 1731, 1373, and 1237 cm⁻¹; ¹³C and ¹H NMR data (see Table 3); ESIMS *m/z* 387 [M + Na]⁺; HRESIMS *m/z* 387.2504 [M + Na]⁺ (calcd for C₂₂H₃₆O₄Na, 387.2506).

Compound 12: Colorless oil; $[\alpha]_D^{24} + 57.0$ (*c* 14.3, CHCl₃); IR (neat) v_{\max} 3496, 2927, 2937, 1736, 1640, 1442, 1373, and 1027 cm⁻¹; ¹H NMR (CDCl₃, 400 MHz): δ_H 5.80 (1H, dd, *J* = 17.6, 10.4 Hz, H-8), 5.48 (1H, dd, *J* = 7.2, 7.2 Hz, H-15), 4.89 (1H, d, *J* = 17.6 Hz, H-9a), 4.89 (1H, d, *J* = 10.4 Hz, H-9b), 4.85 (1H, dd, *J* = 9.2, 4.0 Hz, H-17), 4.81 (1H, s, H-11a), 4.66 (1H, d, *J* = 12.0 Hz, H-14a), 4.58 (1H, d, *J* = 12.0 Hz, H-14b), 4.56 (1H, s, H-11b), 2.46, (2H, m, H-6, H₂-16), 2.06 (3H, s, 17-OCOCH₃), 2.05 (3H, s, 14-OCOCH₃) 2.03, (1H, m, H-4), 1.99 (1H, dd, *J* = 11.6, 3.6 Hz, H-2), 1.69 (3H, s, H₃-12), 1.53, (2H, m, H₂-5), 1.49 (2H, m, H₂-3), 1.41 (2H, m, H₂-6), 1.22 (6H, s, H₃-19 and H₃-20), 0.98 (3H, s, H₃-7); ¹³C NMR (CDCl₃, 100 MHz): δ_C 171.0 (C, 14-OCOCH₃), 170.6 (C, 17-OCOCH₃), 150.0 (CH, C-8), 147.4 (C, C-10), 140.7 (C, C-13), 125.6 (CH, C-15), 112.2 (CH₂, C-11), 110.0 (CH₂, C-9), 78.9 (CH, C-17), 72.1 (C, C-18), 61.1 (CH₂, C-14), 52.6 (CH, C-2), 43.7 (CH, C-4), 39.8 (CH₂, C-6), 39.7 (C, C-1), 33.1 (CH₂, C-3), 28.2 (CH₂, C-16), 27.1 (CH₂, C-5), 26.5 (CH₃, C-19), 25.3 (CH₃, C-20), 24.8 (CH₃, C-12), 21.1 (CH₃, 14-OCOCH₃), 20.9 (CH₃, 17-OCOCH₃), 16.5 (CH₃, C-7); ESIMS *m/z* 429 [M + Na]⁺; HRESIMS *m/z* 429.2609 [M + Na]⁺ (calcd for C₂₄H₃₈O₅Na, 429.2612).

Compound 13: Colorless oil; $[\alpha]_D^{24} - 81.0$ (*c* 1.4, CHCl₃); IR (neat) v_{\max} 3254, 2925, 2857, 1640, 1450, and 1023 cm⁻¹; ¹H NMR (CDCl₃, 500 MHz): δ_H 6.50 (1H, dd, *J* = 15.5, 11.0 Hz, H-13), 5.90 (1H, d, *J* = 11.0 Hz, H-12), 5.78 (1H, d, *J* = 15.5 Hz, H-14), 5.29 (1H, s, H-3), 4.58 (1H, dd, *J* = 7.0, 7.0 Hz, H-1), 3.55 (1H, dd, *J* = 7.0, 7.0 Hz, H-1), 2.31 (1H, m, H-2a), 1.98 (2H, m, H-2b and H-7), 1.95 (1H, m, H-5), 1.92 (1H, m, H-9a), 1.71 (1H, m, H-6a), 1.80 (3H, s, H₃-18), 1.60 (2H, m, H₂-8), 1.58 (3H, s, H₃-16), 1.36 (6H, s, H₃-19 and H₃-20), 1.29 (1H, m, H-6b), 1.14 (1H, m, H-9b), 0.79 (3H, s, H₃-17); ¹³C NMR (CDCl₃, 125 MHz): δ_C 143.6 (C, C-11), 139.3 (CH, C-14), 135.2 (C, C-4), 123.0 (CH₂, C-13), 122.7 (CH, C-12), 119.5 (CH, C-3), 76.4 (CH, C-1), 71.0 (C, C-15), 52.8 (CH₂, C-2), 48.0 (CH, C-7), 46.6 (CH, C-5), 37.4 (C, C-10), 35.0 (CH₂, C-9), 29.9 (2 × CH₃, C-19 and C-20), 28.2 (CH₂, C-6), 26.0 (CH₂, C-8), 20.8 (CH₃, C-16), 15.0 (CH₃, C-18), 9.5 (CH₃, C-17); ESIMS *m/z* 327 [M + Na]⁺; HRESIMS *m/z* 327.2296 [M + Na]⁺ (calcd for C₂₀H₃₂O₂Na, 327.2295).

Preparation of (S)- and (R)-MTPA Esters of 1

To a solution of **1** (1.0 mg, 3.1 μmol) in anhydrous pyridine (200 μL) was added S-(+)- α -methoxy- α -(trifluoromethyl)phenylacetyl (MTPA) chloride (20 μL), and the mixture was further reacted for 20 h at room temperature. The reaction mixture was then processed as previously described [20,21] to yield the (R)-MTPA ester **1a** (0.5 mg, 0.93 μmol, 30%). The correspondent (S)-MTPA ester **1b** was similarly yielded from the reaction of R-(−)-MTPA chloride with **1**. ¹H NMR (CDCl₃, 400 MHz) of **1a**: δ_H 5.8005 (1H, dd, *J* = 17.6, 10.4 Hz, H-8), 4.892 (1H, d, *J* = 12 Hz, H-9b), 5.114 (1H, dd,

$J = 5.6, 5.6$ Hz, H-17), 4.8895 (1H, d, $J = 16.4$ Hz, H-9a), 4.822 (1H, s, H-11b), 4.591 (1H, s, H-11a), 3.949 (1H, dd, $J = 8.4, 6.8$ Hz, H-15), 2.395 (1H, ddd, $J = 10.0, 6.8, 6.8$ Hz, H-16b), 1.994 (1H, m, H-16a), 1.9475 (1H, m, H-2), 1.708 (3H, s, H₃-12), 1.689 (1H, d, $J = 15.2$, H-3b), 1.522 (1H, m, H-3a), 1.367 (1H, m, H-4), 1.394–1.229 (4H, m, H₂-5 and H₂-6), 1.279 (3H, s, H₃-20), 1.210 (3H, s, H₃-14), 1.158 (3H, s, H₃-19), 0.981 (3H, s, H₃-7); ¹H NMR (CDCl₃, 400 MHz) of **1b**: δ_{H} 5.803 (1H, dd, $J = 17.6, 10.4$ Hz, H-8), 4.895 (1H, d, $J = 12$ Hz, H-9b), 5.136 (1H, dd, $J = 6.0, 6.0$ Hz, H-17), 4.8945 (1H, d, $J = 16.4$ Hz, H-9a), 4.883 (1H, s, H-11b), 4.605 (1H, s, H-11a), 3.971 (1H, dd, $J = 8.0, 7.6$ Hz, H-15), 2.419 (1H, ddd, $J = 9.6, 6.8, 6.8$ Hz, H-16b), 2.107 (1H, m, H-16a), 1.989 (1H, m, H-2), 1.718 (3H, s, H₃-12), 1.7665 (1H, br d, $J = 14.0$, H-3b), 1.5325 (1H, m, H-3a), 1.415 (1H, m, H-4), 1.394–1.256 (4H, m, H₂-5 and H₂-6), 1.236 (3H, s, H₃-20), 1.198 (3H, s, H₃-14), 1.106 (3H, s, H₃-19), 0.995 (3H, s, H₃-7).

3.4. Cytotoxic Testing

Cytotoxicities of **1–11** were assayed using Almar Blue assay [25,26]. Doxorubicin HCl, employed as positive control, displayed cytotoxic activity toward DLD-1, HT-29, HuCCT-1, and P388 cell lines with IC₅₀ 0.9, 4.4, 2.6, and 7.4 $\mu\text{g/mL}$, respectively.

3.5. In Vitro Anti-Inflammatory Testing

The experiment for measuring superoxide anion generation and elastase release were manipulated according to previously reported method [28,32,33].

4. Conclusions

In conclusion, our further chemical investigation and biological evaluation on the EtOAc extract of the soft coral *L. varium* disclosed three new lobane and eight prenyleudesmane diterpenoids along with two known derivatives. Compound **1** is the first labane possessing a tetrahydrofuran ring at the end of the side chain, and displayed ability to inhibit elastase release in the absence of fMLF/CB. Compounds **2**, **4**, **12**, and **13**, in particular **12** and **13**, displayed the potential to be the leads for anti-inflammatory medicines. Our proposed stereospecific biosynthetic pathway can explain the common coexistence of both lobanes and prenyleudesmanes in the soft coral *L. varium*.

Supplementary Materials: HRESIMS, ¹H, ¹³C, COSY, heteronuclear single quantum coherence spectroscopy (HSQC), HMBC, and NOESY spectra of new compounds **1–11** and ¹H NMR spectrum of MTPA ester of **1** are available online at <http://www.mdpi.com/1660-3397/18/4/223/s1>, Figure S1: HRESIMS spectrum of **1**, Figure S2: ¹H NMR spectrum of **1** in CDCl₃ at 400 MHz, Figure S3: ¹³C NMR spectrum of **1** in CDCl₃ at 100 MHz, Figure S4: ¹H-¹H COSY spectrum of **1** in CDCl₃, Figure S5: HSQC spectrum of **1** in CDCl₃, Figure S6: HMBC spectrum of **1** in CDCl₃, Figure S7: NOESY spectrum of **1** in CDCl₃, Figure S8: ¹H NMR spectrum of (*S*)-MTPA ester of **1** (**1a**) in CDCl₃ at 400 MHz, Figure S9: ¹H NMR spectrum of (*R*)-MTPA ester of **1** (**1b**) in CDCl₃ at 400 MHz, Figure S10: HRESIMS spectrum of **2**, Figure S11: ¹H NMR spectrum of **2** in CDCl₃ at 400 MHz, Figure S12: ¹³C NMR spectrum of **2** in CDCl₃ at 100 MHz, Figure S13: ¹H-¹H COSY spectrum of **2** in CDCl₃, Figure S14: HSQC spectrum of **2** in CDCl₃, Figure S15: HMBC spectrum of **2** in CDCl₃, Figure S16: NOESY spectrum of **2** in CDCl₃, Figure S17: HRESIMS spectrum of **3**, Figure S18: ¹H NMR spectrum of **3** in CDCl₃ at 500 MHz, Figure S19: ¹³C NMR spectrum of **3** in CDCl₃ at 125 MHz, Figure S20: ¹H-¹H COSY spectrum of **3** in CDCl₃, Figure S21: HSQC spectrum of **3** in CDCl₃, Figure S22: HMBC spectrum of **3** in CDCl₃, Figure S23: NOESY spectrum of **3** in CDCl₃, Figure S24: HRESIMS spectrum of **4**, Figure S25: ¹H NMR spectrum of **4** in CDCl₃ at 400 MHz, Figure S26: ¹³C NMR spectrum of **4** in CDCl₃ at 100 MHz, Figure S27: ¹H-¹H COSY spectrum of **4** in CDCl₃, Figure S28: HSQC spectrum of **4** in CDCl₃, Figure S29: HMBC spectrum of **4** in CDCl₃, Figure S30: NOESY spectrum of **4** in CDCl₃, Figure S31: HRESIMS spectrum of **5a** and **5b**, Figure S32: ¹H NMR spectrum of **5a** and **5b** acetone-*d*₆ at 500 MHz, Figure S33: ¹³C NMR spectrum of **5a** and **5b** in acetone-*d*₆ at 125 MHz, Figure S34: ¹H-¹H COSY spectrum of **5a** and **5b** in acetone-*d*₆, Figure S35: HSQC spectrum of **5a** and **5b** in acetone-*d*₆, Figure S36: HMBC spectrum of **5a** and **5b** in acetone-*d*₆, Figure S37: NOESY spectrum of **5a** and **5b** in acetone-*d*₆, Figure S38: HRESIMS spectrum of **6**, Figure S39: ¹H NMR spectrum of **6** in CDCl₃ at 400 MHz, Figure S40: ¹³C NMR spectrum of **6** in CDCl₃ at 100 MHz, Figure S41: ¹H-¹H COSY spectrum of **6** in CDCl₃, Figure S42: HSQC spectrum of **6** in CDCl₃, Figure S43: HMBC spectrum of **6** in CDCl₃, Figure S44: NOESY spectrum of **6** in CDCl₃, Figure S45: HRESIMS spectrum of **7**, Figure S46: ¹H NMR spectrum of **7** in CDCl₃ at 400 MHz, Figure S47: ¹³C NMR spectrum of **7** in CDCl₃ at 100 MHz, Figure S48: ¹H-¹H COSY spectrum of **7** in CDCl₃, Figure S49: HSQC spectrum of **7** in CDCl₃, Figure

S50: HMBC spectrum of **7** in CDCl₃, Figure S51: NOESY spectrum of **7** in CDCl₃, Figure S52: HRESIMS spectrum of **8**, Figure S53: ¹H NMR spectrum of **8** in CDCl₃ at 400 MHz, Figure S54: ¹³C NMR spectrum of **8** in CDCl₃ at 100 MHz, Figure S55: ¹H-¹H COSY spectrum of **8** in CDCl₃, Figure S56: HSQC spectrum of **8** in CDCl₃, Figure S57: HMBC spectrum of **8** in CDCl₃, Figure S58: NOESY spectrum of **8** in CDCl₃, Figure S59: HRESIMS spectrum of **9**, Figure S60: ¹H NMR spectrum of **9** in CDCl₃ at 400 MHz, Figure S61: ¹³C NMR spectrum of **9** in CDCl₃ at 100 MHz, Figure S62: ¹H-¹H COSY spectrum of **9** in CDCl₃, Figure S63: HSQC spectrum of **9** in CDCl₃, Figure S64: HMBC spectrum of **9** in CDCl₃, Figure S65: NOESY spectrum of **9** in CDCl₃, Figure S66: HRESIMS spectrum of **10**, Figure S67: ¹H NMR spectrum of **10** in CDCl₃ at 500 MHz, Figure S68: ¹³C NMR spectrum of **10** in CDCl₃ at 125 MHz, Figure S69: ¹H-¹H COSY spectrum of **10** in CDCl₃, Figure S70: HSQC spectrum of **10** in CDCl₃, Figure S71: HMBC spectrum of **10** in CDCl₃, Figure S72: NOESY spectrum of **10** in CDCl₃, Figure S73: HRESIMS spectrum of **11**, Figure S74: ¹H NMR spectrum of **11** in CDCl₃ at 500 MHz, Figure S75: ¹³C NMR spectrum of **11** in CDCl₃ at 125 MHz, Figure S76: ¹H-¹H COSY spectrum of **11** in CDCl₃, Figure S77: HSQC spectrum of **11** in CDCl₃, Figure S78: HMBC spectrum of **11** in CDCl₃, Figure S79: NOESY spectrum of **11** in CDCl₃.

Author Contributions: J.-H.S. designed and guided the whole experiment; C.-H.C. and T.-S.Y. isolated the compounds and performed structure elucidation; A.F.A. and Y.-C.L. performed structure elucidation and manuscript preparation; C.-Y.H. performed cytotoxicity assay; T.-L.H. performed the anti-inflammatory activity assay. All authors have read and agreed to the published version of the manuscript.

Funding: The research was funded by the Ministry of Science and Technology of Taiwan (MOST 102-2628-B-110-002-MY2, 104-2320-B-110-001-MY2, 105-2113-M-110-002- and 105-2811-M-110-013-) and the Deanship of Scientific Research at King Saud University, Saudi Arabia (RG-1440-127).

Acknowledgments: This work was mainly supported by grants from Ministry of Science and Technology (MOST 102-2628-B-110-002-MY2, 104-2320-B-110-001-MY2, 105-2113-M-110-002- and 105-2811-M-110-013-) awarded to J.-H.S., A.F.A. would like to extend appreciation to the Deanship of Scientific Research at King Saud University for further funding this work through research group RG-1440-127.

Conflicts of Interest: The authors declare no conflicts of interest.

References

1. Ahmed, A.F.; Teng, W.T.; Hung, C.Y.; Dai, C.F.; Hwang, T.L.; Sheu, J.H. Anti-inflammatory lobane and prenyleudesmane diterpenoids from the soft coral *Lobophytum varium*. *Mar. Drugs* **2017**, *15*, 300. [[CrossRef](#)] [[PubMed](#)]
2. Edrada, R.A.; Proksch, P.; Wray, V.; Witte, L.; van Ofwegen, L. Four new bioactive lobane diterpenes of the soft coral *Lobophytum pauciflorum* from Mindoro, Philippines. *J. Nat. Prod.* **1998**, *61*, 358–361. [[CrossRef](#)] [[PubMed](#)]
3. Dunlop, R.W.; Wells, R.J. Isolation of some novel diterpenes from a soft coral of the genus *Lobophytum*. *Aust. J. Chem.* **1979**, *32*, 1345–1351. [[CrossRef](#)]
4. Lakshmana Raju, B.; Subbaraju, G.V.; Bheemasankara Rao, C.; Trimurtulu, G. Two new oxygenated lobanes from a soft coral of *Lobophytum* species of the Andaman and Nicobar coasts. *J. Nat. Prod.* **1993**, *56*, 961–966. [[CrossRef](#)]
5. Hamada, T.; Kusumi, T.; Ishitsuka, M.O.; Kakisawa, H. Structures and absolute configurations of new lobane diterpenoids from the Okinawan soft coral *Simularia flexibilis*. *Chem. Lett.* **1992**, *21*, 33–36. [[CrossRef](#)]
6. Govindam, S.V.; Yoshioka, Y.; Kanamoto, A.; Fujiwara, T.; Okamoto, T.; Ojika, M. Cyclobatriene, a novel prenylated germacrene diterpene, from the soft coral *Lobophytum pauciflorum*. *Bioorg. Med. Chem.* **2012**, *20*, 687–692. [[CrossRef](#)]
7. Minh, C.V.; Kiem, P.V.; Nhiem, N.X.; Cuong, N.X.; Thao, N.P.; Nam, N.H.; Anh, H.L.T.; Thung, D.C.; Thuy, D.T.T.; Kang, H.K.; et al. Cytotoxic and antioxidant activities of diterpenes and sterols from the Vietnamese soft coral *Lobophytum compactum*. *Bioorg. Med. Chem. Lett.* **2011**, *21*, 2155–2159. [[CrossRef](#)]
8. Li, L.; Sheng, L.; Wang, C.Y.; Zhou, Y.B.; Huang, H.; Li, X.B.; Li, J.; Mollo, E.; Gavagnin, M.; Guo, Y.W. Diterpenes from the Hainan soft coral *Lobophytum cristatum* Tixier-Durivault. *J. Nat. Prod.* **2011**, *74*, 2089–2094. [[CrossRef](#)]
9. Coll, J.C.; Bowden, B.F.; König, G.M.; Braslau, R.; Price, I.R. Studies of Australian soft corals. XXXX.1 The natural products chemistry of Alcyonacean soft corals with special reference to the genus *Lobophytum*. *Bull. Soc. Chim. Belg.* **1986**, *95*, 815–834. [[CrossRef](#)]
10. Matthee, G.F.; König, G.M.; Wright, A.D. Three new diterpenes from the marine soft coral *Lobophytum crassum*. *J. Nat. Prod.* **1998**, *61*, 237–240. [[CrossRef](#)]

11. Bowden, B.F.; Coll, J.C.; Liyanage, N.; Mitchell, S.J.; Stokie, G.J.; van Altena, I. A novel bicyclic diterpene was obtained from a soft coral *Lobophytum hedleyi*. *Aust. J. Chem.* **1978**, *31*, 163–170. [[CrossRef](#)]
12. Chao, C.H.; Wen, Z.H.; Wu, Y.C.; Yeh, Y.C.; Sheu, J.H. Cytotoxic and anti-inflammatory cembranoids from the soft coral *Lobophytum crassum*. *J. Nat. Prod.* **2008**, *71*, 1819–1824. [[CrossRef](#)] [[PubMed](#)]
13. Lee, N.L.; Su, J.H. Tetrahydrofuran cembranoids from the cultured soft coral *Lobophytum crassum*. *Mar. Drugs* **2011**, *9*, 2526–2536. [[CrossRef](#)]
14. Roy, P.K.; Roy, S.; Ueda, K. New cytotoxic cembranolides from an Okinawan soft coral, *Lobophytum* sp. *Fitoterapia* **2019**, *136*, 104162. [[CrossRef](#)] [[PubMed](#)]
15. Rashid, M.A.; Gustafson, K.R.; Boyd, M.R. HIV-inhibitory cembrane derivatives from a Philippines collection of the soft coral *Lobophytum* species. *J. Nat. Prod.* **2000**, *63*, 531–533. [[CrossRef](#)] [[PubMed](#)]
16. Kao, C.Y.; Su, J.H.; Lu, M.C.; Hwang, T.L.; Wang, W.H.; Chen, J.J.; Sheu, J.H.; Kuo, Y.H.; Weng, C.F.; Fang, L.S.; et al. New cembrane-type diterpenoids from the soft coral *Lobophytum crassum*. *Mar. Drugs* **2011**, *9*, 1319–1331. [[CrossRef](#)] [[PubMed](#)]
17. Lai, K.H.; You, Y.J.; Lin, C.C.; El-Shazly, M.; Liao, Z.J.; Su, J.H. Anti-Inflammatory cembranoids from the soft coral *Lobophytum crassum*. *Mar. Drugs* **2017**, *15*, 327. [[CrossRef](#)]
18. Thao, N.P.; Luyen, B.T.T.; Ngan, N.T.T.; Song, S.B.; Cuong, N.X.; Nam, N.H.; Kiem, P.V.; Kim, Y.H.; Minh, C.V. New anti-inflammatory cembranoid diterpenoids from the Vietnamese soft coral *Lobophytum crassum*. *Bioorg. Med. Chem. Lett.* **2014**, *24*, 228–232. [[CrossRef](#)]
19. Kusumi, T.; Hamada, T.; Ishitsuka, M.O.; Ohtani, I.; Kakisawa, H. Elucidation of the relative and absolute stereochemistry of lobatriene, a marine diterpene, by a modified Mosher method. *J. Org. Chem.* **1992**, *57*, 1033–1035. [[CrossRef](#)]
20. Peng, C.-C.; Huang, C.-Y.; Ahmed, A.F.; Hwang, T.-L.; Dai, C.-F.; Sheu, J.-H. New cembranoids and a biscebranoid peroxide from the soft coral *Sarcophyton cheronnieri*. *Mar. Drugs* **2018**, *16*, 276. [[CrossRef](#)]
21. Ohtani, I.; Kusumi, T.; Kashman, Y.; Kakisawa, H. High-Field FT NMR application of Mosher's Method. The absolute configurations of marine terpenoids. *J. Am. Chem. Soc.* **1991**, *113*, 4092–4096. [[CrossRef](#)]
22. Hiroyuki, K.; Satoshi, T.; Shun-ichi, T.; Yoshihara, T.; Sakamura, S.; Shimanuki, T.; Sato, T.; Tajimi, A. New fungitoxic sesquiterpenoids, chokols A-G, from stromata of *Epichloe typhina* and the absolute configuration of chokol E. *Agric. Biol. Chem.* **1989**, *53*, 789–796. [[CrossRef](#)]
23. Pérez Morales, C.; Catalán, J.; Domingo, V.; González Delgado, J.A.; Dobado, J.A.; Herrador, M.M.; Quílez del Moral, J.F.; Barrero, A.F. Protecting-group-free synthesis of chokols. *J. Org. Chem.* **2011**, *76*, 2494–2501. [[CrossRef](#)] [[PubMed](#)]
24. Shin, J.; Fenical, W. Fuscoides A-D: Anti-inflammatory diterpenoid glycosides of new structural classes from the caribbean gorgonian *Eunicea fusca*. *J. Org. Chem.* **1991**, *56*, 3153–3158. [[CrossRef](#)]
25. O'Brien, J.; Wilson, I.; Orton, T.; Pognan, F. Investigation of the Alamar Blue (resazurin) fluorescent dye for the assessment of mammalian cell cytotoxicity. *Eur. J. Biochem.* **2000**, *267*, 5421–5426. [[CrossRef](#)]
26. Nakayama, G.R.; Caton, M.C.; Nova, M.P.; Parandoosh, Z. Assessment of the Alamar Blue assay for cellular growth and viability in vitro. *J. Immunol. Methods* **1997**, *204*, 205–208. [[CrossRef](#)]
27. Hwang, T.L.; Yeh, S.H.; Leu, Y.L.; Chern, C.Y.; Hsu, H.C. Inhibition of superoxide anion and elastase release in human neutrophils by 3'-isopropoxychalcone via a cAMP-dependent pathway *Br. J. Pharmacol.* **2006**, *148*, 78–87.
28. Hwang, T.L.; Su, Y.C.; Chang, H.L.; Leu, Y.L.; Chung, P.J.; Kuo, L.M.; Chang, Y.J. Suppression of superoxide anion and elastase release by C18 unsaturated fatty acids in human neutrophils. *J. Lipid Res.* **2009**, *50*, 1395–1408. [[CrossRef](#)]
29. De Kraker, J.W.; Franssen, M.C.R.; de Groot, A.; König, W.A.; Bouwmeester, H.J. (+)-Germacrene a biosynthesis: The committed step in the biosynthesis of bitter sesquiterpene lactones in chicory. *Plant Physiol.* **1998**, *117*, 1381–1392. [[CrossRef](#)]
30. Cheng, S.Y.; Chuang, C.T.; Wang, S.K.; Wen, Z.H.; Chiou, S.F.; Hsu, C.H.; Dai, C.F.; Duh, C.Y. Antiviral and anti-inflammatory diterpenoids from the soft coral *Simularia gyrosa*. *J. Nat. Prod.* **2010**, *73*, 1184–1187. [[CrossRef](#)]
31. Ye, F.; Zhu, Z.D.; Gu, Y.C.; Li, J.; Zhu, W.L.; Guo, Y.W. Further New Diterpenoids as PTP1B Inhibitors from the Xisha Soft Coral *Simularia polydactyla*. *Mar. Drugs* **2018**, *16*, 103. [[CrossRef](#)] [[PubMed](#)]

32. Yang, S.C.; Chung, P.J.; Ho, C.M.; Kuo, C.Y.; Hung, M.F.; Huang, Y.T.; Chang, W.Y.; Chang, Y.W.; Chan, K.H.; Hwang, T.L. Propofol inhibits superoxide production, elastase release, and chemotaxis in formyl peptide-activated human neutrophils by blocking formyl peptide receptor 1. *J. Immunol.* **2013**, *190*, 6511–6519. [[CrossRef](#)] [[PubMed](#)]
33. Yu, H.P.; Hsieh, P.W.; Chang, Y.J.; Chung, P.J.; Kuo, L.M.; Hwang, T.L. 2-(2-Fluorobenzamido)benzoate ethyl ester (EFB-1) inhibits superoxide production by human neutrophils and attenuates hemorrhagic shock-induced organ dysfunction in rats. *Free Radic. Biol. Med.* **2011**, *50*, 1737–1748. [[CrossRef](#)] [[PubMed](#)]



© 2020 by the authors. Licensee MDPI, Basel, Switzerland. This article is an open access article distributed under the terms and conditions of the Creative Commons Attribution (CC BY) license (<http://creativecommons.org/licenses/by/4.0/>).